Fast Algorithm for Vectorcardiogram and Interbeat Intervals Analysis: Application for Premature Ventricular Contractions Classification

Irena Jekova, Vessela Krasteva[∗]

Centre of Biomedical Engineering "Prof. Ivan Daskalov" - Bulgarian Academy of Sciences
105 Acad. G. Bonchev Str., 1113 Sofia, Bulgaria
E-mail:irena@clbme.bas.bg, vessika@clbme.bas.bg
[∗] Corresponding author

Abstract: *In this study we investigated the adequacy of two non-orthogonal ECG leads from Holter recordings to provide reliable vectorcardiogram (VCG) parameters. The VCG loop was constructed using the QRS samples in a fixed-size window around the fiducial point. We developed an algorithm for fast approximation of the VCG loop, estimation of its area and calculation of relative VCG characteristics, which are expected to be minimally dependent on the patient individuality and the ECG recording conditions. Moreover, in order to obtain independent from the heart rate temporal QRS characteristics, we introduced a parameter for estimation of the differences of the interbeat RR intervals. The statistical assessment of the proposed VCG and RR interval parameters showed distinguishing distributions for N and PVC beats. The reliability for PVC detection of the extracted parameter set was estimated independently with two classification methods - a stepwise discriminant analysis and a decision-tree-like classification algorithm, using the publicly available MIT-BIH arrhythmia database. The accuracy achieved with the stepwise discriminant analysis presented sensitivity of 91% and specificity of 95.6%, while the decision-tree-like technique assured sensitivity of 93.3% and specificity of 94.6%. We suggested possibilities for accuracy improvement with adequate electrodes placement of the Holter leads, supplementary analysis of the type of the predominant beats in the reference VCG matrix and smaller step for VCG loop approximation.*

Keywords: *Heartbeat Classification, Holter ECG Leads, VCG loop, RR intervals.*

Introduction

The automatic analysis of the electrocardiogram (ECG) has become a standard tool for fast diagnostics of different cardiac dysfunctions by computer-based algorithms for detection of different heartbeat types. The occurrence of multiple abnormal cardiac contractions associated with excitation from ectopic center in the ventricles (known as premature ventricular contractions (PVC) or ventricular extrasystols) is considered clinically important, since it is a sign for disturbance in the depolarization process preceding in many cases the appearance of malignant cardiac arrhythmia [15]. The problem for automatic detection of PVCs is widely discussed in the literature and usually the rules for automatic heartbeat classification are based on the specific features of the QRS complex, being the most significant wave in the ECG. In comparison to the normally exited beats, the PVCs have wider QRS complex (>0.12s) and bizarre waveforms due to the abnormal prolongation of the conduction path through the ventricles. The study of the interbeat RR intervals shows that the single PVC appears earlier than the normal RR interval, followed by a prolonged RR-interval (usually complete compensatory pause, rarely incomplete compensatory pause), or it may appear sandwiched in between two normal beats (the so called interpolated PVCs).

Automated heartbeat classification was traditionally performed using the morphological descriptors of the QRS waveform [1, 2, 4, 5, 8, 10, 12], as well as the RR intervals [2, 14]. In some works, these parameters were processed with relatively complicated methods as neural networks [4, 7, 14], linear discriminants using likelihood functions [2], operation on vectors in the multidimensional space [5, 12], etc. Obviously, the performance of the morphological and the temporal QRS descriptors has been extensively studied and highly optimized. In contrast, the spatial behavior of the cardiac electrical vector, represented by the vectorcardiogram (VCG), has not been widely investigated in the aspect of PVC detection, except in the works of few authors [1,3,4,5,8]. It could be expected that the PVC vectorcardiographic loops differ in shape and orientation from the normal QRS loops in the Frank orthogonal leads. Using Holter recorders, however, the researchers face the limitation of ECG signal acquisition from a small number of chest electrodes, which are not sufficient for reconstruction of independent orthogonal VCG leads. Aiming to overcome this limitation, Chia et al. [3] used two ECG leads acquired from four chest electrodes placed over the heart in a cross orientation, thus achieving single-plane VCG projection, which is close to the orthogonal one. The authors then applied a VCG-based triggering algorithm for effective rejection of PVC beats. Another studies for PVC recognition [4, 5] investigated the performance of two VCG parameters (the magnitude of the maximal vector and its angle) calculated for the non-orthogonal leads of the publicly available MIT-BIH arrhythmia ECG database [11]. Although the PVC detection accuracy with patient-specific local learning set was promising [4], the training with a global learning set reduced the accuracy [8]. A point of interest becomes the investigation of Holter non-orthogonal VCG leads and extraction of VCG parameters, which are independent from the shape and orientation of the VCG-loop among the individuals.

In this study we investigated the relations between the area spatial displacements of the VCG loops for N and PVC beats in the two non-orthogonal ECG leads from Holter recordings available in the MIT-BIH database. We propose an algorithm for fast approximation of the VCG loop and calculation of its area. By estimation of the common area with a constructed reference VCG loop, we introduce relative VCG characteristics, which are expected to be minimally dependent on the patient individuality and the ECG recording conditions. Moreover, we include a relative assessment of the temporal heartbeat characteristics by calculation the differences of the interbeat RR intervals. A discriminant analysis and a decision-tree-like approach are applied for assessment of the PVC classification ability of the proposed VCG and RR interval parameters.

Materials and Method
ECG Signals
The study involved all 48 ECG recordings from the MIT-BIH arrhythmia database. The recordings were digitized at 360 samples per second per channel with 11-bit resolution over a 10 mV range. Each recording has a duration of 30 min and includes two leads – 42 recordings with the modified limb lead II and V1, 3 recordings with the modified II and V5 (100, 114, 123), 2 recordings with V2 and V5 (102, 104), 1 recording with the modified lead II and V4 (124) [9]. The heartbeats were recognized by the fiducial points in the database and the original database annotations were taken into account. Since we focused only on the PVC classification, we accepted two heartbeat groups – Normal (N) group and PVC group. The N group is a kind of summary group, which included: (i) all beats, which were annotated as Normals (approximately 70% of all beats in the database); (ii) some types of abnormal beats, which are predominant in the patient recording (left and right bundle branch blocks and paced

beats); (iii) premature atrial contractions. We excluded from the study all remaining heartbeat types, which comprise about 2% of all beats in the database, including: aberrantly conducted beats, nodal premature beats, nodal or atrial premature beats, nodal escape beats, nodal ectopic beats, atrial ectopic beats, fusion premature ventricular contractions, ventricular flutter waves, ventricular escape beats, blocked atrial premature beats, missed beats and questionable beats. In addition, we avoided the processing of all low amplitude heartbeats (<150μV from peak-to-peak in one of the ECG leads), since the low-amplitude signals corrupt the VCG loop to the point that the analysis is compromised. In future real-time implementation, monitoring of the ECG signal amplitude is expected. In case of low amplitude detection for more than 10s in one of the ECG channels, an alarm for bad electrode contact has to be generated. Thus, the presence of Holter ECG data with compromised quality is directed to the operator's attention. On the other hand, the appearance of short duration event of PVCs with low amplitude projection in one of the leads would not disable the heartbeat analysis.

Preprocessing

The applied digital filtering prevents against power-line interference, tremor noise and base-line drift distortions of the input ECG signal that impede the accurate measurement and classification of the heartbeats. The implemented preprocessing filtration procedures have been accepted previously in [4] and have the advantage for real-time operation. The following procedures are realized:

- a notch filter for elimination of the power-line interference, implemented by moving averaging of samples in one period of the interference;
- a low-pass filter for suppression of the tremor noise, realized by moving averaging of samples in 30 ms time-interval, thus having a first zero at about 35 Hz;
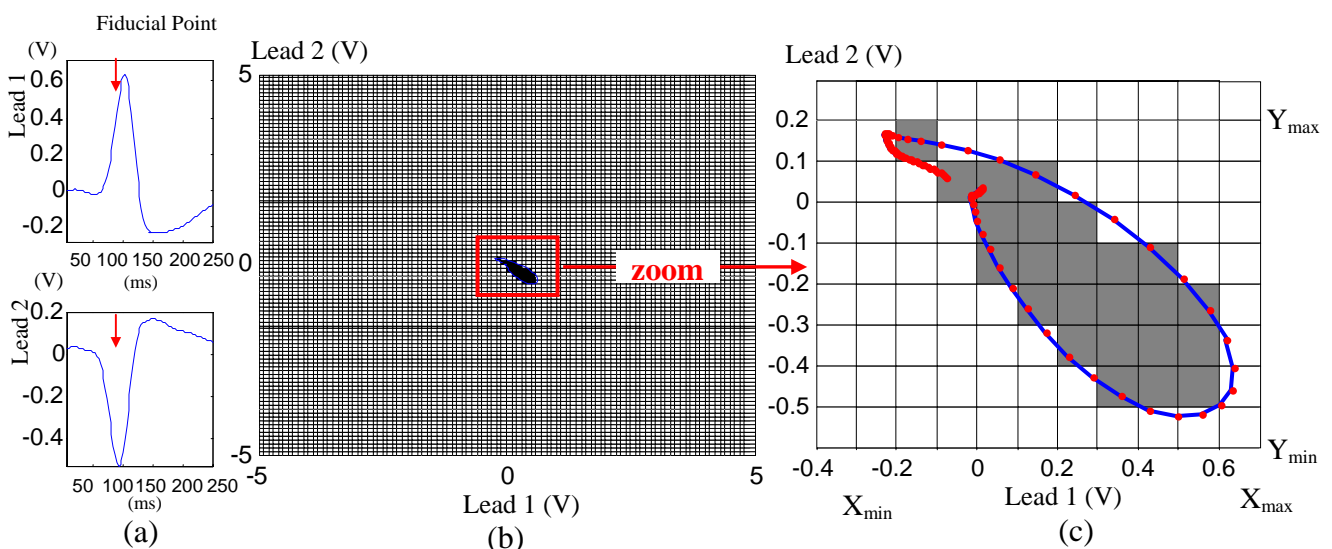- a high-pass recursive filter for drift suppression [6] with cut-off frequency of 2.2 Hz.

Fig.1. Illustration of 2-lead ECG and the single-plane VCG loop approximation.
(a) - Lead1 and Lead2: The extracted QRS segment of fixed size around the fiducial point;
(b) - VCG plane: Division in square regions with a side of 100μV. The VCG-loop of the selected QRS complex is drawn and highlighted by the red square.
(c) - Zoomed view of the approximated VCG loop: the approximated area is drawn with grey squares (correspond to the *VCGMatrix$_{TEST}$* elements with value 1). The original VCG loop samples are marked with (•).

VCG analysis
Extraction of the QRS complex
The heartbeats were extracted in segments of 90 samples (250 ms) with the fiducial point at the 30th sample. Thus, the window of fixed-size around the fiducial point (about 80 ms before and 160 ms after) guarantees the selection of the complete QRS wave, even in the worst case of prolonged ventricular extrasystole. An illustration of the two ECG leads representing the extracted QRS segment and the position of the fiducial point is shown in Fig. 1a.

Calculation of VCG Matrix of the tested QRS complex
We introduce the VCG Matrix as an approximation of the VCG loop spatial position, aiming to facilitate the associated calculations. For the sake of the approximation, the VCG plane, formed by Lead1 and Lead2 is divided in square regions having a side of 100μV. Thus, a number of 100x100 squares fill the entire VCG plane, taking into account the minimal and the maximal ECG signal amplitude of –5V and +5V, respectively (Fig. 1b). All squares form the *VCGMatrix_{TEST}* (size 100x100) and they could take a value 0 or 1, in dependence on the spatial position of the VCG loop of the tested QRS complex. The *VCGMatrix_{TEST}* elements are assigned as follows:

- Initialization – all elements are set to 0;
- Selection of the *VCGMatrix_{TEST}* elements, which belong to the rectangle defined by [X_{min}, X_{max}, Y_{min}, Y_{max}],
  where $X_{min} = \min(Lead1); X_{max} = \max(Lead1); Y_{min} = \min(Lead2); X_{max} = \max(Lead2);$
- Each of the selected *VCGMatrix_{TEST}* elements is tested whether it is internal or it is external for the VCG loop. We apply a fast algorithm [13], which calculates the number of crossings of the ray between an internal point for the VCG loop and the element center (coordinates X_c, Y_c), according to Condition (1). The odd number of crossings indicates an outside element (value set to 0), while the even number indicates an inside element (value set to 1). An example of calculated *VCGMatrix_{TEST}* elements is presented in Fig. 1c.

$$\left| \begin{array}{l} (Lead2_i \leq Y_c \text{ and } Y_c < Lead2_j) \text{ or } (Lead2_j \leq Y_c \text{ and } Y_c < Lead2_i) \\ \\ \text{and } X_c < \dfrac{Lead1_j - Lead1_i}{Lead2_j - Lead2_i}(Y_c - Lead2_i) + Lead1_i \end{array} \right. \qquad , \qquad (1)$$

where i, j are the consecutive indexes of the VCG loop samples ($i = \overline{1,2,...N}; j = \overline{N,1,2,....N-1}$).

Calculation of Reference VCG Matrix
The reference VCG Matrix (*VCGMatrix_{REF}*) is calculated as a mean of the VCG Matrixes of the five previous QRS complexes, according to Equation (2). The values of its elements are rounded towards the nearest integer and are equal either to 0 or to 1. Thus, the reference VCG Matrix has ones only in these elements, which represent VCG loop spatial distribution repeated in 3 or more QRS complexes from the 5 reference beats. The example of ECG signal with N and PVC beats (see Fig. 2a) represents the calculated reference VCG Matrix involving beats with indexes from T-5 to T-1 (see Fig. 2b). It is evident that the black area (the ones in the reference VCG Matrix) coincides with the elements, which are internal for at least three VCG loops.

$$VCGMatrix_{REF} = round(\frac{\sum_{i=T-5}^{T-1}VCGMatrix_i}{5}) ,$$ (2)

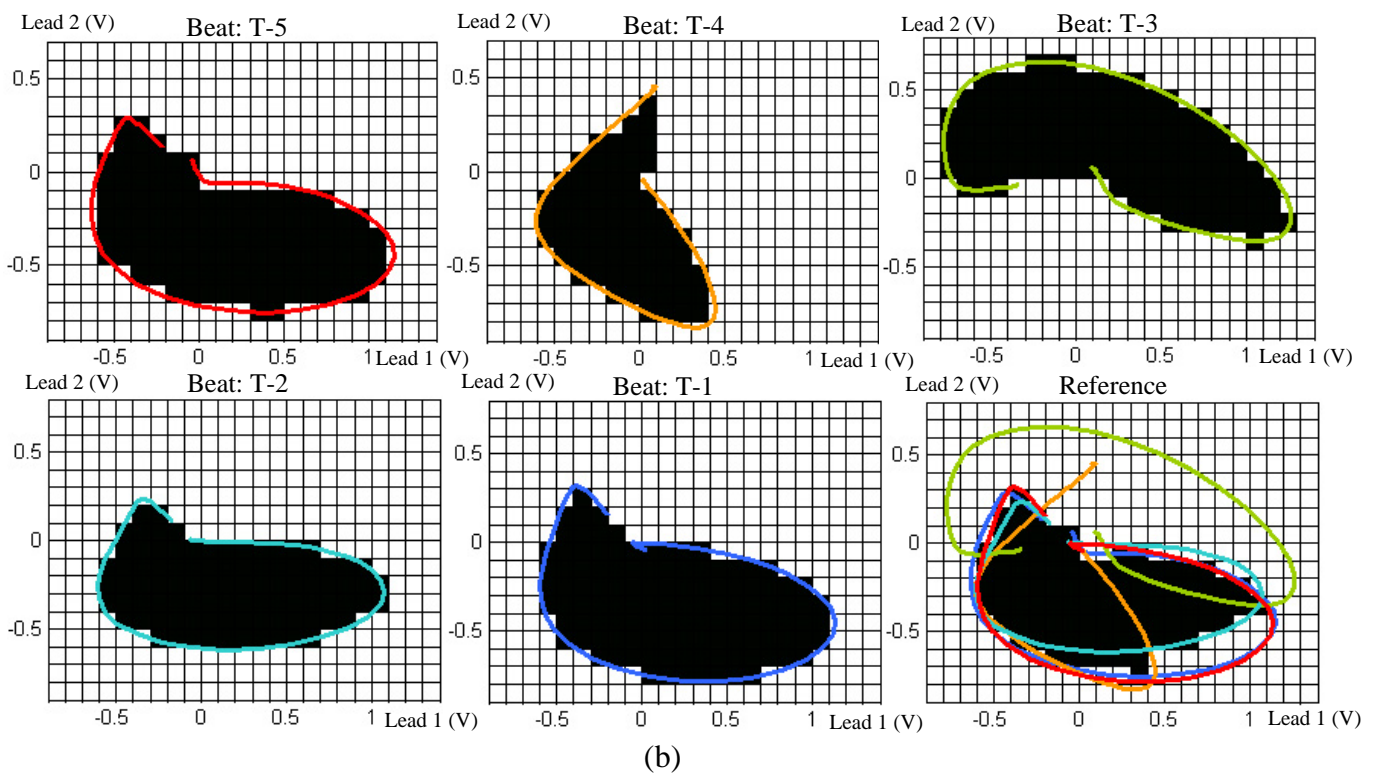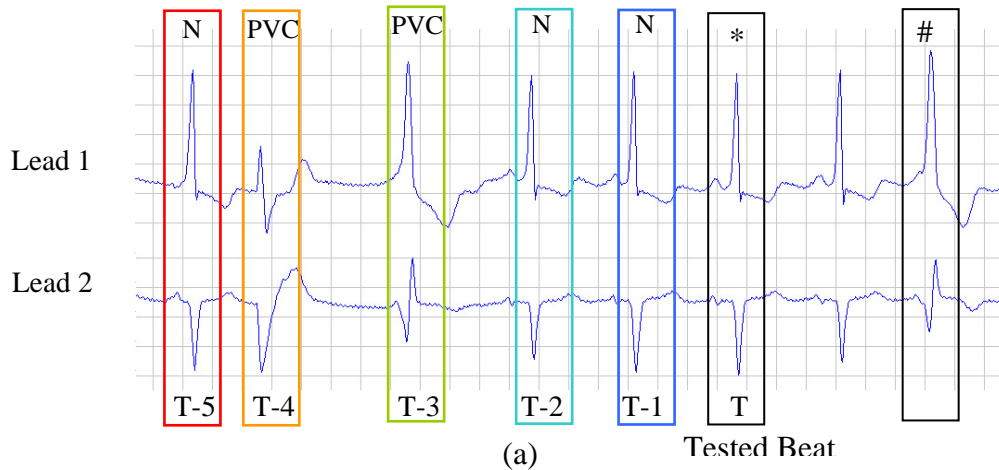where T is the consecutive index of the tested QRS-complex in the file.

Fig.2. Illustration of the reference *VCG Matrix* calculation
(a) - Example of ECG signal with N and PVC beats.
(b) - The VCG loops and their approximated areas for the beats with indexes from T-5 to T-1.
The last subplot illustrates the calculated reference *VCG Matrix*, which summarizes the
VCG loop spatial distributions of all five QRS complexes.

Calculation of Common VCG Matrix

We introduce the Common VCG Matrix (*VCGMatrix$_{COMMON}$*) for estimation of the area of overlapping between the reference VCG Matrix and the VCG Matrix of the tested QRS complex. Since the matrixes elements are binary (0 or 1), their common parts could be easily calculated with logical AND, as written in Equation (3).

$$VCGMatrix_{COMMON} = VCGMatrix_{REF} \, \& \, VCGMatrix_{TEST} \hspace{3cm} (3)$$

Fig. 3 is an illustration of the Common VCG Matrix (grey squares) placed over the reference VCG Matrix and the VCG Matrix of the tested QRS complex (black squares + grey squares). It is well seen that in case of N beat, the reference VCG Matrix (Fig. 3a) and the tested VCG Matrix (Fig. 3b) overlap with more than 80%. In case of PVC beat, the Common VCG Matrix fills less than 30% of both the reference VCG Matrix (Fig. 3c) and of the tested VCG Matrix (Fig. 3d).
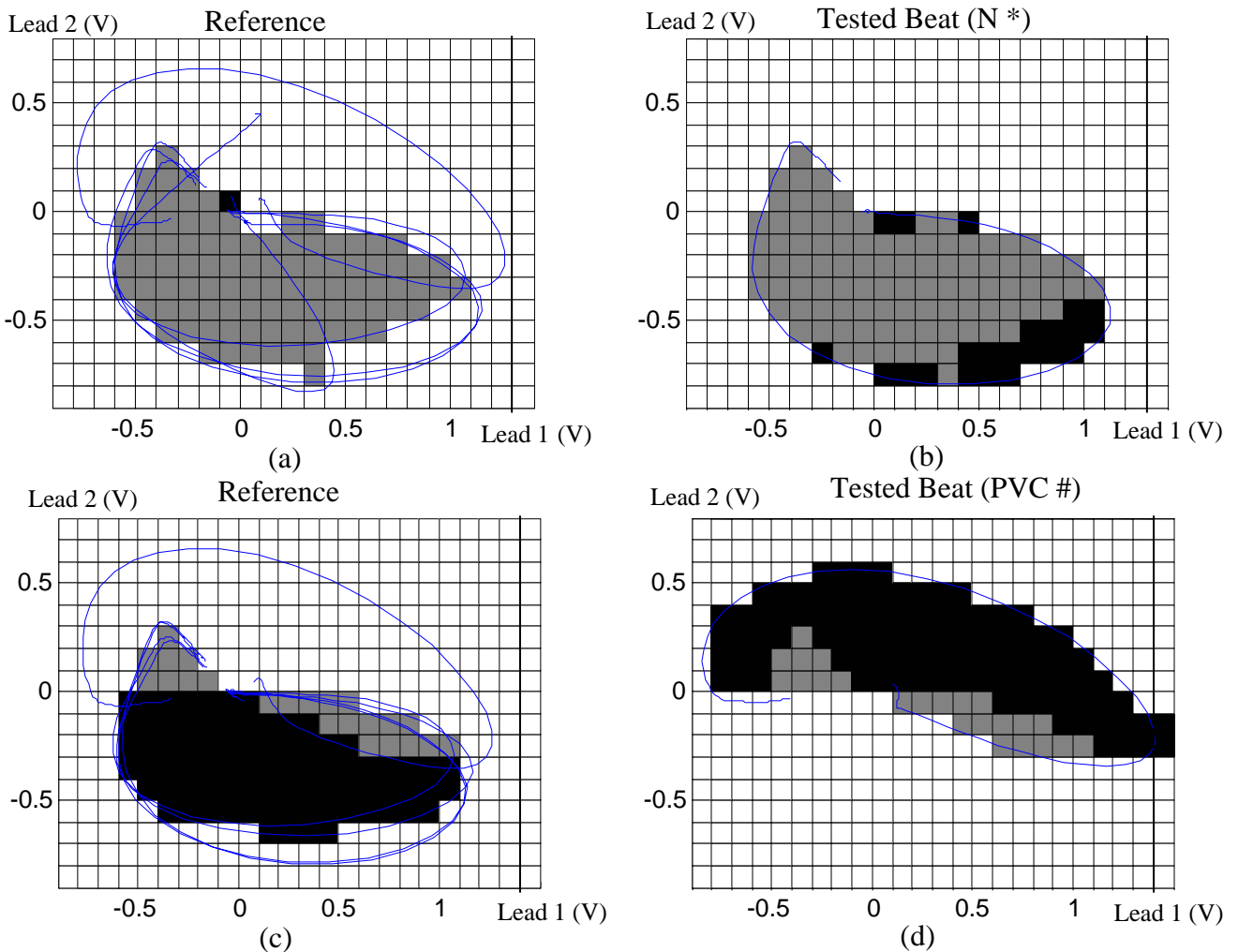

Fig.3. Illustration of the common *VCG Matrix* calculation. The Common VCG Matrix is shown with grey squares, placed over the black squares of the reference VCG Matrix (a,c) and the VCG Matrix of the tested QRS complex (b,d).
(a,b) – The tested QRS complex is N beat (marked with * in Fig.2a)
(c,d) – The tested QRS complex is PVC beat (marked with # in Fig.2a)

Calculation of VCG parameters

We estimate the VCG areas, defined by the introduced above VCG matrixes as the sum of their elements, presented in Equation (4):

$$VCGArea = \sum_{x=X\min}^{X\max} \sum_{y=Y\min}^{Y\max} VCGMatrix(x, y) , \tag{4}$$

where: $VCGMatrix = VCGMatrix_{TEST}, VCGMatrix_{REF}, VCGMatrix_{COMMON}$;

$X_{\min} = \min(Lead1)$; $X_{\max} = \max(Lead1)$; $Y_{\min} = \min(Lead2)$; $X_{\max} = \max(Lead2)$;

These VCG areas are greatly dependent on the ECG recording conditions, which for example influence the ECG signal amplitude. Thus, the values of the calculated areas may differ even for one and the same patient, which makes them incomparable. In order to provide relative VCG characteristics, which are expected to be minimally dependent on the patient individuality and the ECG recording conditions, we introduce the relative VCG parameters, named *DA* and *DB*, calculated according to Equations (5) and (6):

$$DA = \frac{VCGArea_{TEST} + VCGArea_{REF} - 2VCGArea_{COMMON}}{VCGArea_{TEST} + VCGArea_{REF}} \tag{5}$$

$$DB = \frac{1}{2}\left(\frac{VCGArea_{COMMON}}{VCGArea_{TEST}} + \frac{VCGArea_{COMMON}}{VCGArea_{REF}}\right) \tag{6}$$

Interbeat RR intervals

The interbeat RR intervals are involved in the computation of the parameter *RRDiff*, which represents the difference between the durations of the two RR intervals, surrounding the tested heartbeat (with index T). The normalization towards the mean value of the previous five consecutive RR intervals is applied, in order to achieve a value independent from the heart rate.

$$RRDiff_T = \frac{RR_T - RR_{T-1}}{\left(\sum_{i=T-7}^{T-2} RR_i\right)/5} .100\,(\%) , \tag{7}$$

where $RR_T = $ *Fiducial Point$_{T+1}$ - Fiducial Point$_T$*

$RR_{T-1} = $ *Fiducial Point$_T$ -Fiducial Point$_{T-1.}$*

Beat classification

Stepwise discriminant analysis

Stepwise discriminant analysis was applied on the defined above parameters *RRDiff*, *DA* and *DB* to differentiate between N and PVC beats. Two linear discriminant functions of the *n*-dimensional vector *x* (*n*=3) were calculated – *F'*(Equation 8) and *F''*(Equation 9).

$$F'(x) = \sum_{i=1}^{n} w_i' x_i + a' \qquad\qquad (8)$$

$$F''(x) = \sum_{i=1}^{n} w_i'' x_i + a'' \qquad\qquad (9)$$

Here w_i', w_i'' and a', a'' are the corresponding discriminant coefficients and constants. F' relates to the possibility the heartbeat described by vector x to be N, while F'' gives the possibility to be PVC. These two discriminant functions were computed for the tested heartbeat and it was labeled as corresponding to one of the two classes: N or PVC, depending on the higher value among F' and F''.

Decision-tree-like classification algorithm
We defined several conditions, which are applied consecutively for classification of the tested heartbeat as N or PVC. The analysis is based on the defined parameters *RRDiff*, *DA* and *DB* and includes the following steps:
- **Step 1**: If (*RRDiff*<-50%) the QRS is classified as N;
- **Step 2**: If (*DA*<0.5) AND (*RRDiff*<20%) the QRS is classified as N;
- **Step 3**: If (*DA*≥0.5) AND (*RRDiff*≥20%) the QRS is classified as PVC;
- **Step 4**: If (*DB*<0.5) the QRS is classified as PVC;
- **Step 5**: If (0.65<*DB*<0.85) AND (25%<*RRDiff*<70%) the QRS is classified as PVC;
- **Step 6**: If (*DA*>0.7) the QRS is classified as PVC;
- **Step 7**: If (*DA*>0.3) AND (*RRDiff*>80%) the QRS is classified as PVC;
- **Step 8**: Else the QRS is classified as N.

The values of the thresholds for *RRDiff*, *DA* and *DB* were chosen by descriptive statistical analysis of the parameters distributions, as shown below in section Results, followed by iterative testing of the detection accuracy and adjusting the threshold values.

Results
All procedures, including the ECG signals preprocessing, the VCG analysis algorithm and the RR intervals differences measurement, were implemented in software utility, using the software package MATLAB 7.0. The computed parameters *RRDiff*, *DA* and *DB* for all beats in the MIT-BIH database were analysed with STATISTICA 6.0 software.

The reliability for PVC detection of the parameters *RRDiff*, *DA* and *DB* was estimated independently with two classification methods - the discriminant analysis and the decision-tree-like approach. The accuracy was evaluated with the statistical indices Sensitivity (*Se*) and Specificity (*Sp*), calculated as follows:

$$Se = \frac{Correctly\ Detected\ PVC\ beats}{Total\ Number\ of\ PVC\ beats} \qquad\qquad (10)$$

$$Sp = \frac{Correctly\ Detected\ N\ beats}{Total\ Number\ of\ N\ beats} \qquad\qquad (11)$$

The results achieved with the stepwise discriminant analysis, which includes at each step the highest ranked parameter, are presented in Table 1.

Table 1. Stepwise discriminant analysis – specificity (Sp), sensitivity(Se) and discriminant functions F'(N beats) and F''(PVC beats) on each step.

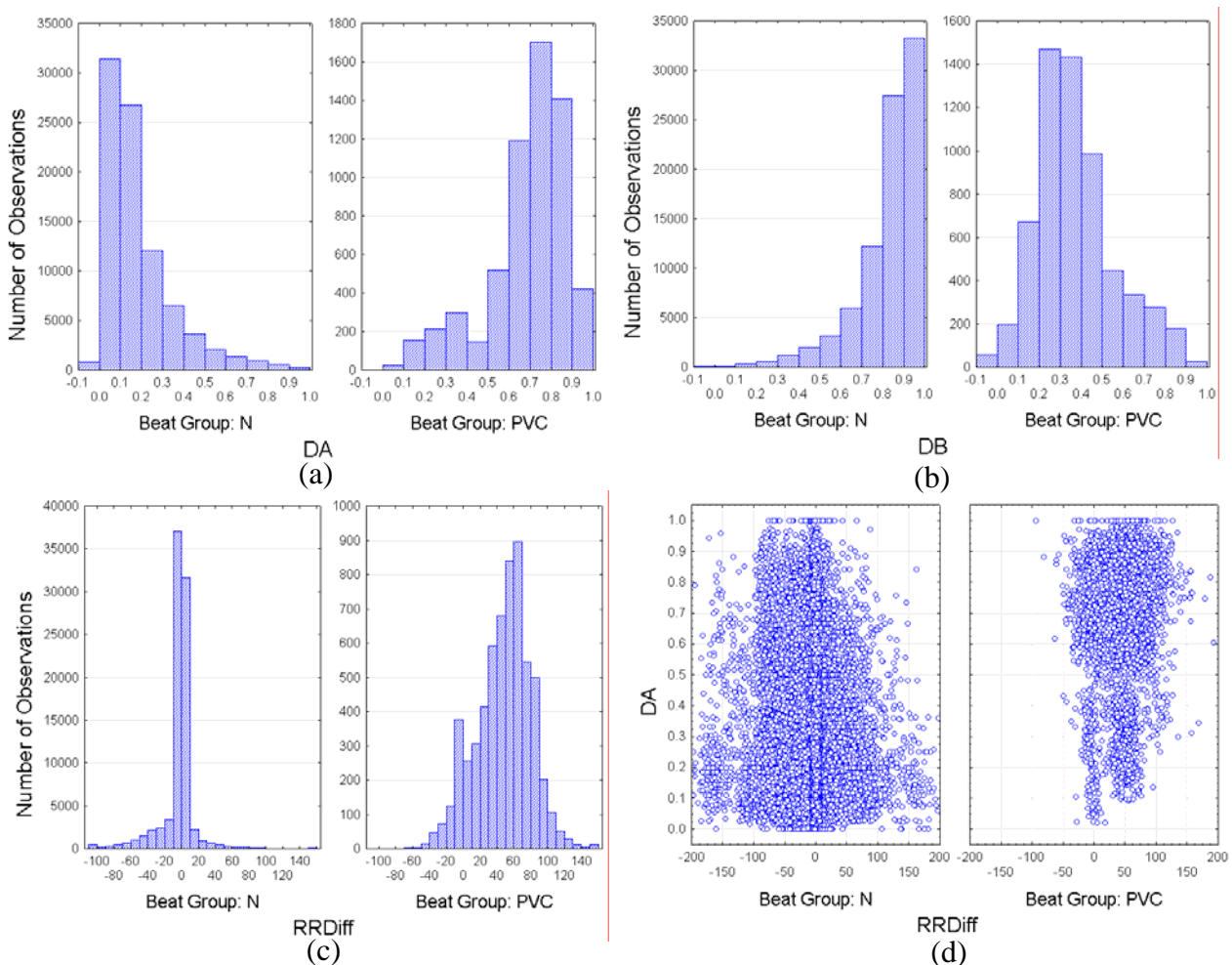| Step	Parameters	Sp(%)	Se(%)	F' (for N beats)	F'' (for PVC beats)
1	DA	91.3	87.4	6.68*DA-1.32	24.46*DA-9.12
2	DA, RRDiff	95.6	91	6.65*DA-0.00232*RRDiff-1.32	25.9*DA+0.11*RRDiff-12.29
3	DA, RRDiff, DB	95.6	90.7	1120*DA+0.098*RRDiff+1225*DB-611	1148*DA+0.213*RRDiff+1235*DB-632

Fig.4. Categorized distributions of the parameters: (a) *DA*, (b) *DB*, (c) *RRDiff* and (d) Scatterplot *DA- RRDiff*, for the two heartbeat groups - N and PVC.

The decision-tree-like algorithm was designed in accordance with the results from the statistical analysis of the parameters *RRDiff*, *DA* and *DB*, which were assessed for all beats in the database. The estimated statistical distributions for the two categories of N and PVC beats are presented in Fig. 4. They were used as a basis for setting the decision rules and the efficacy of each step is presented in Table 2.

Table 2. The percent of correctly and erroneously classified N and PVC beats estimated towards the total number of N and PVC beats at each step of the decision-tree-like algorithm.

	Step 1	Step 2	Step 3	Step 4	Step 5	Step 6	Step 7	Step 8
True N	3.6%	87.6%	-	-	-	-	-	3.4%
False N	-	-	0.4%	3.9%	0.9%	0.03%	0.09%	-
True PVC	-	-	69.6%	14.5%	7.3%	1.1%	0.8%	-
False PVC	0.1%	3%	-	-	-	-	-	3.6%

The total accuracy achieved with the decision-tree-like classification approach is shown in Table 3. The best results, which were attained at the second step of the discriminant analysis, are also added for comparison.

Table 3. Specificity (Sp) and sensitivity(Se) obtained with the discriminant analysis (second step) and the decision-tree-like classification method.

Classification Method	Sp(%)	Se(%)
Discriminant analysis (DA, RRDiff)	95.6	91
Decision-tree-like method	94.6	93.3

Discussion

The study was focused on the widely discussed problem for automatic discrimination between normal and premature ventricular contractions. We investigated the projection of the cardiac electrical vector on the single-plane formed by two Holter chest leads, aiming to find out significant differences between the VCG loops of the N and the PVC beats in one patient. Since the analysis of the spatial correlation of two VCG loops is associated with time-consuming and relatively complicated mathematical procedures, we applied an approach for approximation of the VCG loops, thus reducing the complexity to operations with binary matrixes. The size of the introduced VCG matrix defines the step of approximation. In our study, the operation with matrixes 100x100 is suggested to be a rational compromise between complexity and accuracy. Thus, we can apply a relatively fast algorithm for searching the VCG matrix elements, which are internal for the VCG loop, and then easily calculate the corresponding VCG loop area. Moreover, we proposed an approach for relative assessment of the spatial displacement of the tested VCG loop area from the position of a reference VCG loop area. The calculated VCG area parameters are minimally dependent on the patient individuality and the ECG recording conditions and, therefore, their statistical comparison for all beats in the database becomes reasonable. We should mention that the number of QRS complexes, which are involved in the estimation of the reference VCG loop, depends on the available memory, speed and computation resources when quasi-real time operation is expected. In our study, a number of five consecutive beats for the reference VCG matrix proved to be appropriate.

The proposed algorithm for PVC detection, which relies on fast VCG analysis, uses fixed-size window of 250ms around the fiducial point for the VCG loop construction. Thus, we guarantee that the selected ECG segment contains the high amplitude QRS complex samples, which specify the most significant part of the VCG loop area. The advantage of this approach is that we avoid the complicated procedures for finding the onsets and the offsets of the ECG waves.

The VCG analysis itself does not contain information about the temporal ECG characteristics. In order to obtain independent from the heart rate temporal QRS characteristics, we introduced a parameter for relative assessment of the interbeat RR intervals differences. The simple calculation of this parameter corresponds to the concept for quasi-real time operation of the algorithm.

The statistical assessment of the proposed VCG and RR interval parameters showed distinguishing distributions for N and PVC beats (see Fig. 4). As expected, the parameter *DA* (Fig. 4a), summarizing the areas of the reference VCG loop and the tested VCG loop, which are outside their common area, has predominantly low values for the N beats (<0.3) and high values for the PVC beats (>0.5), for more than 80% of the cases. The parameter *DB* (Fig. 4b), which estimates the ratio between the common area and the size of both the reference VCG loop and the tested VCG loop, feature with high values for the N beats (>0.7) and relatively low values for the PVC beats (<0.7). This proved the assumption that the N-beats being the predominant beats in the calculation of the reference VCG loop matrix, would repeat the spatial VCG loop distribution of a tested N-beat (see Fig.3 a,b) and just in opposite, the reference VCG loop would be highly distinguishable from a casual PVC beat (see Fig.3 c,d). The more complicated cardiac dysfunctions associated with frequent alteration of N or PVC beats (more than 3 PVCs in a number of 5 consecutive beats), would lead to calculus of a reference VCG matrix with predominant PVC loops, that could mislead the values of *DA* and *DB* parameters typical for N and PVC beats. We consider that a supplementary analysis of the type of the predominant beats in the reference VCG matrix would improve the accuracy by classifying the tested beat as belonging or not to the type of the predominant beats in the reference set.

The analysis of the RR intervals shows that the parameter *RRDiff* (Fig. 4c) has well expressed peak between –20% and +20% for the N beats, which appear normally in regular RR intervals. In contrast, the PVC beats have wider *RRDiff* distribution, resulting from the variety of PVCs with complete compensatory pause, non-complete compensatory pause or lack of compensatory pause. Moreover, we should take into account that the *RRDiff* parameter has similar values for the ventricular and the atrial premature contractions, the last being part from the N group.

The discriminant analysis classified the VCG descriptor *DA* as the top-ranked parameter in the studied parameter set (see Table 1). The use of *RRDiff* in combination with *DA* improved the accuracy to 95.6% in recognition of N beats and 91% in recognition of PVC beats. The discriminant analysis was unable to provide better results when including the second VCG parameter *DB*. The designed decision-tree-like classification algorithm operates together with *DA*, *DB* and *RRDiff* parameters, and achieves more balanced results with specificity of 94.6% and sensitivity of 93.3%. The results do not outmatch the reported accuracy of other methods for heartbeat classification, but there are several factors, which might influence the performance of the analyzed parameters. For example, the Holter MIT-BIH database was collected with different combinations of chest leads, which obviously changed the projections of the electrical vector on the relevant VCG planes. Thus, the relation between the spatial displacements of the VCG loops for N and PVC beats could vary - in some leads being very enhanced, while in others being hardly visible. Therefore, the use of Holter electrodes placement, which ensures almost independent orthogonal VCG leads, is a potential approach for improvement of the reliability of the studied VCG parameters. Another action towards results improvement is the use of smaller step for VCG loop approximation, which however is associated with large VCG matrixes and more heavy computation procedures.

Conclusion

We proposed an approach for PVC detection from 2 non-orthogonal Holter leads, which was based on a fast algorithm for VCG loop analysis and interbeat RR intervals differences calculation. The performed statistical assessment of the extracted parameter set proved the potential ability of the VCG loop and RR intervals analyses to provide a reliable tool for PVC classification in Holter ECG recordings. We suggested possibilities for accuracy improvement with adequate electrodes placement of the Holter leads, supplementary analysis of the type of the predominant beats in the reference VCG matrix and smaller step for VCG loop approximation.

References

1. Bortolan G., I. Jekova, I. Christov (2005). Comparison of four methods for premature ventricular contractions and normal beats clustering, Computers in Cardiology, 32 (in press).
2. Chazal P., M. O'Dwyer, R. B. Reilly (2004). Automatic classification of heartbeats using ECG morphology and heartbeat interval features, IEEE Transaction on Biomedical Engineering, 51, 1196–1206.
3. Chia J. M., S. E. Fischer, S. A. Wickline, C. H. Lorenz (2000). Performance of QRS detection for cardiac magnetic resonance imaging with a novel vectorcardiographic triggering method, Journal of Magnetic Resonance Imaging, 12 (5), 678-688.
4. Christov I., G. Bortolan (2004). Ranking of pattern recognition parameters for premature ventricular contraction classification by neural networks, Physiological Measurement, 25, 1281-1290.
5. Christov I., I. Jekova, G. Bortolan (2005). Premature ventricular contraction classification by the Kth nearest neighbours rule, Physiological Measurement, 26, 123-130.
6. Daskalov I. K., I. A. Dotsinsky, I. Christov (1998). Developments in ECG acquisition, preprocessing, parameter measurement and recording, IEEE Engineering in Medicine & Biology, 17, 50-58.
7. Gómez-Herrero G., A. Gotchev, I. Christov, K. Egiazarian (2005). Heartbeat classification using independent component analysis and matching pursuits, IEEE, Int. Conf. Acoustics, Speech and Signal Processing, ICASSP, Philadelphia, USA, 4, 725-728.
8. Jekova I., G. Bortolan, I. Christov (2004). Pattern recognition and optimal parameter selection in premature ventricular contraction classification, Computers in Cardiology, 31, 357-360.
9. Mark R., G. Moody (1988). MIT-BIH Arrhythmia database directory. Cambridge: Massachusetts Institute of Technology.
10. Millet J., M. Perez, G. Joseph, A. Mocholi, J. Chorro (1997). Previous identification of QRS Onset and Offset is not essential for classifying QRS complex in a single lead, Computers in Cardiology, 24, 299-302.
11. MIT-BIH Arrhythmia database. http://physionet.org/physiobank/database/mitdb.
12. Moreas J., M. O. Seixas, F. N. Vilani, E. V. Costa (2002). A real time QRS complex classification method using Mahalanobis distance, Computers in Cardiology, 29, 201-204.
13. O'Rourke J. Computational Geometry in C, http://cs.smith.edu/~orourke/books/ftp.html.
14. Tsipouras M.G., D.I. Fotiadis, D. Sideris. (2002). Arrhythmia classification using the RR interval duration signal, Computers in Cardiology, 29, 485-488.
15. Wagner S.G. (1994). Marriott's practical electrocardiography, 9-th ed., Williams and Wilkins, Baltimore, Maryland.